Brownian Dynamics Study of Mixed Linear-Hyperbranched Polymers

A. T. Lee and A. J. McHugh*

Department of Chemical Engineering, University of Illinois, Urbana, Illinois 61801

Received February 21, 2001; Revised Manuscript Received July 3, 2001

ABSTRACT: Brownian dynamics simulations have been performed on a variety of mixed linear-branched molecules. The rheological properties of three different constant molecular weight systems, with varying ratios of linear segments to branch points, are reported. The transition from perfectly branched behavior (low viscosity) to linear-chain-like behavior (high viscosity) is found to occur at a mole fraction of linear segments of 0.8.

Introduction

Along with molecular weight and molecular weight distribution, chain architecture has long been known to play an important role in the control of rheological and material properties of polymeric materials. This awareness has led to a renewed interest in recent years in the development of routes for synthesizing molecules with controlled branching and molecular weight. These activities culminated in the recent development of metallocene-synthesized polyolefins[1,2] and the so-called dendritic materials, the latter encompassing perfect dendrimers[3−6] on the one extreme and hyperbranched polymers,[7] or HBP's, on the other. Because of their precise functionality and end group multiplicity, perfect dendrimers are characterized by several attractive properties such as high solubility and low viscosities with respect to conventional linear chain polymers of comparable molecular weights. This has led to their potential use as rheological modifiers and coatings. However, the systematic step by step synthesis of perfect dendrimers is expensive, and large-scale industrial synthesis is not considered viable. Moreover, due to the lack of chain entanglements, these systems exhibit fairly simple Newtonian viscosity behavior in their rheology.[8]

Our own research has focused on HBP's. These are randomly branched structures that, similar to dendrimers, emanate from a central core or focal points with multiple end groups. Hyperbranched polymers are synthesized by a single step polycondensation between AB_f ($f \geq 2$) monomers containing one reactive group (A) and "*f*" reactive groups (B) of another type. While these molecules do not have the well-defined monodisperse topology of perfect dendrimers, they are much more rapidly and economically synthesized, yet by control of their degrees of branching, they can be made to exhibit properties intermediate between perfect dendrimers and conventional linear molecules. Recently, a series of AB/AB_2 polyetherimide copolymers have been synthesized and characterized in our laboratory.[9] The molecular weights of these samples have been maintained relatively constant, while incremental architectural changes have been achieved by varying the ratio of AB to AB_2 monomer units. The primary finding has been that a transition from dendrimer-like properties (low viscosity) to linear-chainlike properties(high viscosity coupled with nonlinear viscoelastic effects) occurs when the mole fraction of linear segment (AB) units in the starting monomer mixture exceeds 0.75. This result has been observed for both dilute and concentrated solutions[10] in NMP (*N*-methylpyrrolidinone).

Over the years, kinetic theories of polymeric solutions have provided considerable insight into the rheological and conformational behavior of polymeric molecules under flow. Most theories have idealized polymer molecules as mechanical models consisting of "beads" connected by "rods" or "springs". Recently we proposed a bead−spring model for perfect dendrimers and investigated their rheology under both shear[11] and extensional flows[12] using nonequilibrium Brownian dynamics (NEBD) simulations. Model predictions were in good qualitative and semiquantitative agreement with experimentally observed behavior. Lyulin et al.[13] have also investigated the simple shear dynamics of perfect dendrimers utilizing a less coarse-grained model. The objective of this paper is to provide insight into the molecular rheology of hyperbranched polymers with the help of kinetic theory models. Since the focus is on the effects of changes in the molecular architecture on the rheology, the effects of excluded volume and hydrodynamic interactions are not considered. While a study on the relative influence of excluded volume effects on the rheology of branched chains is still lacking, for linear chains, solvent quality has been shown to have only a minor influence on the shear viscosity at all shear rates, as well as the extensional viscosity at high extension rates.[14] However, the solvent quality is known to significantly affect the quiescent mean squared radius of gyration. An excellent study on the effects of solvent quality on the quiescent conformational states of perfect dendrimers can be found in the paper by Murat and Grest[15] who showed that, under poor solvent conditions, the radial monomer density distribution shifts toward the core of the dendrimer.

We considered the effects of hydrodynamic interactions (HI) in our previous study of the rheology of perfect dendrimers[12] and found that its inclusion does not significantly influence the overall qualitative trends in either the shear thinning behavior, the intrinsic viscosity−molecular weight dependence, or the extensional flow response. Moreover, it also results in increases in the zero shear viscosities, which are less than 10%.

The two primary issues investigated in this study are (a) the effect of linear spacers on the rheology of the perfectly branched architecture and (b) the effect of the mole fraction of linear segments on the rheology of a series of constant molecular weight hyperbranched systems.

* To whom correspondence should be addressed.

10.1021/ma0103122 CCC: $20.00
Published on Web 08/29/2001

Theory and Methods

The two basic building blocks of the model we have developed are rigid trumbbell units and "Fraenkel" spring units (Figure 1). The trumbbells consist of three identical beads which occupy the vertexes of an equilateral triangle and each of which is a distance L from the center of the trumbbell. The springs are of equilibrium length l_0 and the spring force is governed by a harmonic stretching potential U^S given by

$$U^S = \sum_i \frac{1}{2} a' k_B T(|\mathbf{l}_i| - l_0)^2 \tag{1}$$

where a' is the stretching constant, k_B is Boltzmann's constant, $\mathbf{l}_i$ is the end-to-end vector of the ith link, and T is the temperature. All our calculations are performed for $L = l_0$. The trumbbells are representative of branch points, and the springs represent the linear segments. Since each bead may correspond to an arbitrary number of actual monomer units, those in the trumbbell configuration may be thought of as being an average representation of some fraction of the total number of dendritic units in the chain. Likewise, those bead units connected linearly may be thought of as representing an average of some fraction of the total number of linear units in the molecule. Except for the end units, each bead serves as a joint which permits adjacent trumbbell and spring units to undergo rotational and bending motions unhindered by rotational or bending potentials. Bead−bead, trumbbell−trumbbell, spring−spring, bead−spring, bead−trumbbell, and trumbbell−spring interactions are neglected in our calculations; i.e., the molecule is made up of "phantom" units which can pass through each other.

The methodology of Bird and co-workers[16] is followed for the kinetic theory analysis. The internal configuration of a molecule is specified through a set of $3(N_{spr} + N_{tr})$ independent generalized coordinates, where N_{spr} and N_{tr} are the number of spring and trumbbell units, respectively. Each spring unit has three degrees of freedom, and the associated generalized coordinates are chosen to be the scalar spring length, l_i, and the polar angles θ_i and ϕ_i, $0 \le \theta_i \le \pi$, $0 \le \phi_i < 2\pi$. Each trumbbell unit also has three degrees of freedom, and the associated generalized coordinates are chosen to be the three Euler angles, α_i, β_i, and γ_i, $0 \le \alpha_i < 2\pi$, $0 \le \beta_i \le \pi$, $0 \le \gamma_i < 2\pi$. The Euler angles of the "core" trumbbell unit at the center of the molecule are chosen as the first three generalized coordinates, Q_1, Q_2. and Q_3.

An embedded coordinate system x′−y′−z′ is chosen, whose origin coincides with the center of the core trumbbell. The core trumbbell unit lies in the y′−z′ plane, with one bead along the −z′ axis and the other two beads making angles of + and −60° with the +z′ axis, respectively. The position vectors of the remaining beads are transformed to the embedded coordinate system through the transformation matrixes

$$\mathbf{C} = \begin{pmatrix} \cos\theta_i \cos\phi_i & -\sin\phi_i & \cos\phi_i \sin\theta_i \\ \sin\phi_i \cos\theta_i & \cos\phi_i & \sin\phi_i \sin\theta_i \\ -\sin\theta_i & 0 & \cos\theta_i \end{pmatrix} \tag{2}$$

and

$$\Omega = \begin{pmatrix} \cos\alpha_i \cos\beta_i \cos\gamma_i - \sin\alpha_i \sin\gamma_i & \sin\alpha_i \cos\beta_i \cos\gamma_i + \cos\alpha_i \sin\gamma_i & -\sin\beta_i \cos\gamma_i \\ -\cos\alpha_i \cos\beta_i \cos\gamma_i - \sin\alpha_i \cos\gamma_i & -\sin\alpha_i \cos\beta_i \sin\gamma_i + \cos\alpha_i \cos\gamma_i & \sin\beta_i \sin\gamma_i \\ \cos\alpha_i \sin\beta_i & \sin\alpha_i \sin\beta_i & \cos\beta_i \end{pmatrix} \tag{3}$$

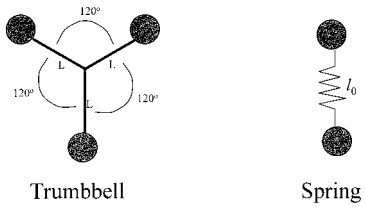

Figure 1. The two basic building blocks of the model: the trumbbell unit and the Fraenkel spring unit.

The transformation from the embedded system to the lab coordinate system is made by utilizing the Ω-matrix of the central trumbbell unit.

The probability of finding the molecule in a given configuration is governed by the distribution function, $\psi(Q_1, Q_2, Q_3, \ldots Q_{3(N_{spr}+N_{tr})})$. The forces acting on a given bead of the molecule are due to hydrodynamic drag, spring stretching, and Brownian motion. Force balance equations for each bead are written and the following simplifying assumptions are made: (i) the hydrodynamic drag on the beads is given by Stoke's law, (ii) the flow is homogeneous, (iii) the acceleration (inertial) terms are neglected in the equation of motion, (iv) the fluid is incompressible, and (v) the velocity distribution is Maxwellian. This yields the diffusion equation (Smoluchowski equation) for the probability distribution function

$$\frac{\partial \psi}{\partial t} = -\sum_t \sum_u \frac{\partial}{\partial Q_t}\left\{ \tilde{G}_{tu}\left[\psi \sum_\nu \frac{\zeta_\nu}{\sqrt{m_\nu}} (\mathbf{K}:\tilde{\mathbf{R}}_\nu \mathbf{b}_{\nu u}) - kT\sqrt{g}\,\frac{\partial}{\partial Q_u}\left(\frac{\psi}{\sqrt{g}}\right) - \left(\frac{\partial \phi}{\partial Q_u}\right)\psi \right] \right\} \tag{4}$$

where the Q_i are the generalized coordinates defined above, $\tilde{\mathbf{R}}_i$ are the position vectors of the beads referred to the center of resistance, $\tilde{G}_{ij}$ are the contravariant metric tensor components, g is the determinant of the covariant metric tensor, and $\mathbf{b}_{ij}$ are the basis vectors referred to the center of mass. m_i are the bead masses and ζ_i are the bead resistances to motion. Since all beads are identical, m_i and ζ_i have constant values of m and ζ respectively. The mathematical definitions of the various quantities can be found elsewhere.[11,16] ϕ is the sum of all the intramolecular potentials (just U^S, in this case). $\mathbf{K}$ is the transpose of the velocity-gradient tensor and is defined as follows

$$\mathbf{K} = \begin{pmatrix} 0 & \dot{\gamma} & 0 \\ 0 & 0 & 0 \\ 0 & 0 & 0 \end{pmatrix} \quad \text{for simple shear flow}$$

$$= \begin{pmatrix} \epsilon & 0 & 0 \\ 0 & (-1/2)\epsilon & 0 \\ 0 & 0 & (-1/2)\epsilon \end{pmatrix} \quad \text{for uniaxial extensional flow} \tag{5}$$

ϕ, $\tilde{\mathbf{R}}_i$, $\tilde{G}_{ij}$, g, $\mathbf{b}_{ij}$ and ψ are all functions of the generalized coordinates, Q_i.

To convert the diffusion equation to its equivalent stochastic differential equation, it is first rewritten in the following form

$$\frac{\partial \psi}{\partial t} = -\frac{\partial}{\partial \mathbf{x}} \cdot (\mathbf{A}(t, \mathbf{x})) + \frac{1}{2}\frac{\partial}{\partial \mathbf{x}}\frac{\partial}{\partial \mathbf{x}}:[\mathbf{D}(t, \mathbf{x})\psi] \quad (6)$$

where

$$\mathbf{x} = (Q_1, Q_2, Q_3, \ldots Q_{3(N_{spr}+N_{tr})} \quad (7)$$

$$\mathbf{D} = 2kT\tilde{\mathbf{G}} \quad (8)$$

$$A_t = \sum_u \tilde{G}_{tu} \sum_\nu \frac{\zeta_\nu}{\sqrt{m_\nu}}(\mathbf{K}:\tilde{\mathbf{R}}_\nu \mathbf{b}_{\nu u}) - \sum_u \tilde{G}_{tu}\left(\frac{\partial \phi}{\partial Q_u}\right) + \sum_u \frac{kT}{\sqrt{g}}\frac{\partial}{\partial Q_u}(\tilde{G}_{tu}\sqrt{g}) \quad (9)$$

The equivalent "Langevin" form, more technically known as the stochastic differential equation(SDE) reads

$$d\mathbf{x} = \mathbf{A}\, dt + \mathbf{B}\cdot d\mathbf{w} \quad (10)$$

where d$\mathbf{w}$ represents a vector of independent Wiener processes and $\mathbf{B}\cdot\mathbf{B}^{\mathbf{T}} = \mathbf{D}$. This equation is forward integrated using an Eulerian scheme

$$\mathbf{x}(t + \Delta t) = \mathbf{x}(t) + \mathbf{A}(t)\Delta t + \mathbf{B}(t)\cdot\Delta\mathbf{w}(t) \quad (11)$$

The elements of $\Delta\mathbf{w}$ represent random displacements with mean zero and variance proportional to the time-step size, Δt. The time-stepping procedure generates a single realization or "trajectory" and the ensemble averages of various properties (such as stress and radius of gyration) are evaluated.

Initial spring lengths are generated using a Monte Carlo acceptance-rejection procedure,[17,18] which utilizes the equilibrium stretching potential energy. Since there are no bending or torsional potentials, the initial angles are generated through random number sampling between 0 and 2π for ϕ_i, α_i and β_i, and between 0 and π for θ_i and β_i. All the equations are nondimensionalized according to the following parameters: (i) stretching constant $a = a'l_0^2$, (ii) time $t^* = tk_BT/\zeta l_0^2$, (iii) shear rate $\gamma^* = \dot{\gamma}\zeta l_0^2/k_BT$, and (iv) extension rate $\epsilon^* = \epsilon\zeta l_0^2/k_BT$. The dimensionless stretching constant is chosen to be 1000 in all our simulations. The simulation protocol for the completely linear chain is described in detail elsewhere.[18]

A dimensionless time step of 1×10^{-4} is found to be optimal and is used in all our simulations. For each time step, an ensemble of 500 to 2000 molecules is used to generate the running averages and variances. Steady-state results are obtained by performing a simulation consisting of a trajectory of 1×10^6 time steps, discarding the initial transient, and performing an average on the remaining time steps. Error bars are obtained from the averaging process and are found to be smaller than the symbols used to represent the data in all cases.

Kramer's expression[16] is used to evaluate the polymer contribution to the stress tensor. where $\tilde{\mathbf{b}}_{ij}$ are the basis vectors referred to the center of resistance and n is the number of molecules.

$$\boldsymbol{\tau}_p = -n\sum_\nu \zeta_\nu\{\langle\tilde{\mathbf{R}}_\nu\tilde{\mathbf{R}}_\nu\rangle\cdot\mathbf{K}^T\} + n\sum_\nu\sum_\mu\sum_t\sum_u\sqrt{\zeta_\nu\zeta_\mu}\{\langle\tilde{G}_{tu}\tilde{\mathbf{R}}_\nu\tilde{\mathbf{b}}_{\nu t}\tilde{\mathbf{b}}_{\mu u}\tilde{\mathbf{R}}_\mu\rangle:\mathbf{K}^T\} + nkT\sum_\nu\sum_t\sum_u\sqrt{\zeta_\nu}\left\langle\frac{1}{\sqrt{g}}\frac{\partial}{\partial Q_u}(\sqrt{g}\tilde{G}_{tu}\tilde{\mathbf{R}}_\nu\tilde{\mathbf{b}}_{\nu t})\right\rangle + n\sum_\nu\sum_t\sum_u\sqrt{\zeta_\nu}\left\langle\tilde{G}_{tu}\left\{\tilde{\mathbf{R}}_\nu\tilde{\mathbf{b}}_{\nu t}\left(-\frac{\partial\phi}{\partial Q_u}\right)\right\}\right\rangle \quad (12)$$

All other quantities are as described before. The viscosity η, the normal stress coefficients Ψ_i, and the extensional viscosity η_E are given by their standard definitions. The intrinsic viscosity is obtained by scaling the viscosity by $nM_w\eta_s/N_A$, where M_w is the molecular weight, η_s is the solvent viscosity and N_A is the Avogadro number.

The radius of gyration tensor, $\langle\mathbf{r}_g^2\rangle$, for any given conformation of the molecule, is given by

$$\langle\mathbf{r}_g^2\rangle = \frac{1}{N}\sum_{i=1}^{N}\langle(\mathbf{r}_i - \mathbf{r}_{cm})(\mathbf{r}_i - \mathbf{r}_{cm})\rangle \quad (13)$$

where $\boldsymbol{r}_i$ denotes the location of the ith bead, $\boldsymbol{r}_{cm}$ denotes the center of mass of the molecule, and N is the total number of beads. The scalar radius of gyration, $\langle R_g^2\rangle$, which is a measure of the average distribution of the molecular mass in the three coordinate directions, is given by the trace of the radius of gyration tensor.

Results and Discussion

To develop a base case for the effects of branching on the rheological response, four "generations" of compact perfectly branched structures were first simulated. The first two generations are shown in Figure 2. The first generation consists of three trumbbell units surrounding the core trumbbell unit, and each subsequent generation has an additional layer of trumbbells. Generations one to four contain 4, 10, 22, and 46 trumbbell units respectively, which correspond to molecular weights (or more correctly, the total number of beads) of 12, 30, 66, and 138. Figure 3 illustrates the shear thinning behavior of the simulated polymer contribution to the total viscosity. A Newtonian plateau is observed at the lower shear rates, and the onset of shear thinning occurs at lower shear rates for the higher generation molecules. The larger molecules are also characterized by a larger asymptotic slope of the viscosity with shear rate, increasing from -0.39 for generation 1 to -0.44 for the generation 3 molecule. These observations are consistent with earlier model studies of perfect dendrimers,[11,13] where the higher generation molecules corresponded to longer relaxation times. The shear rate dependence of the first normal stress coefficients for the four molecules is plotted in Figure 4, and an asymptotic slope of -1.33 is observed for all cases. The shear thinning behavior of the viscosity and first normal stress coefficient appear to be independent of branching, since a similar behavior is found for the Kramer's freely jointed bead−rod chain.[19] It must be noted that our previous studies have shown that including the restriction of bond bending motions through a bending potential can significantly alter molecular deformability and shear thinning behavior.[11,18] However, our interest in the present simulations is to investigate the relative

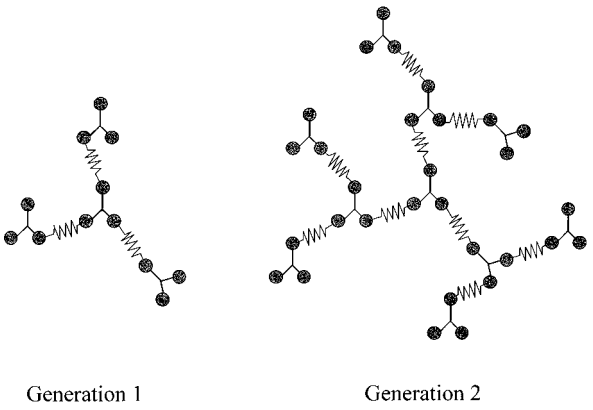

Figure 2. The compact perfectly branched generation 1 and 2 structures.

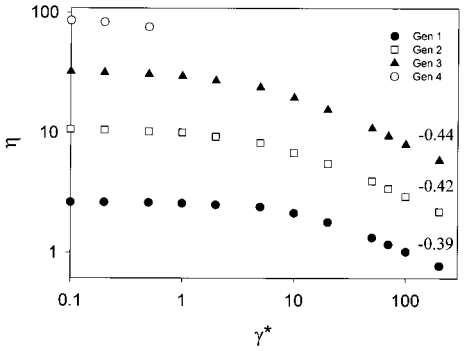

Figure 3. Shear thinning behavior of the viscosity for the four generations of perfectly branched structures.

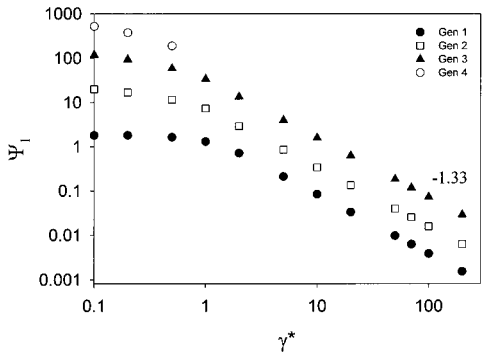

Figure 4. Shear thinning behavior of the first normal stress difference for the four generations of perfectly branched structures.

effects of chain branching through the inclusion of arbitrary numbers of linear units in the chain architecture.

Figure 5 shows the dependence of the zero-shear radius of gyration, R_{g0} on the molecular weight for the four generations of molecules. R_{g0} is evaluated as $\langle R_{g0}^2 \rangle^{1/2}$ and an $M^{0.21}$ dependence is observed at the higher generations. Lescanec and Muthukumar[20] have utilized a kinetic growth algorithm to study the static scaling behavior of perfect dendrimers and have observed an $M^{0.22}$ dependence. Murat and Grest[15] and Lyulin et al.[13] have accounted for the effects of solvent quality through a Lennard-Jones potential and have observed dependencies of $M^{0.33}$ and $M^{0.31}$ respectively. Since we do not consider any excluded volume effects and utilize a random-walk type chain generation scheme, it is to be expected that our coefficient is closer to that predicted by the Muthukumar model.

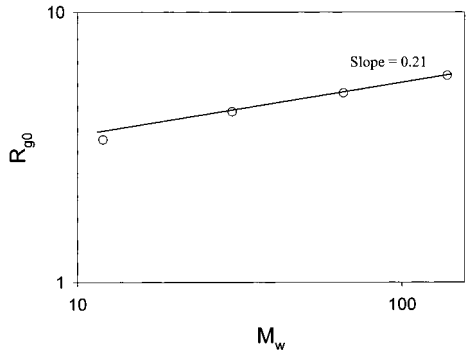

Figure 5. Dependence of zero-shear radius of gyration on the molecular weight. A power law coefficient of 0.21 is obtained, similar to the Muthukumar[20] model.

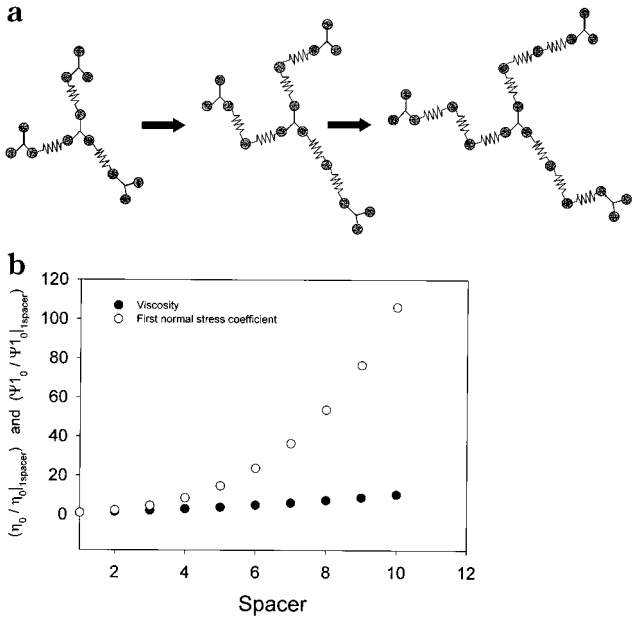

Figure 6. (a) Symmetric addition of linear spacer units in the generation 1 structure. (b) Effect of linear spacers on the zero-shear viscosity and first normal stress difference of the generation 1 molecule.

As a first step toward simulating the effects of varying ratios of linear units to branch points, the number of spring units between the trumbbells was symmetrically increased in the above compact structures. The addition of "linear" spacers is schematically described in Figure 6a, for the generation 1 molecule. The number of spacers was increased from 1 to 10 for the generation 1 and 2 molecules and from 1 to 5 for the generation 3 molecule. The effect of increasing the number of linear units on the zero-shear viscosity and first normal stress coefficient of the generation 1 system is shown in Figure 6b. Similar trends were observed for the generation 2 and 3 systems. Kinetic theory studies of the linear Rouse and Kramer's chains have shown that the zero shear viscosity has a quadratic dependence on the number of links, while the first normal stress coefficient is a much stronger function of the number of links, the leading term being to the fourth power.[21] Likewise, we find that the first normal stress coefficient is more sensitive to the addition of spring units even in the branched systems. Increasing the number of spacers is also found to result in a reduction of the critical shear rate for the onset of shear thinning and an increase in the magnitudes of the asymptotic shear thinning slopes (not shown). The slopes are found to increase from 0.39 to

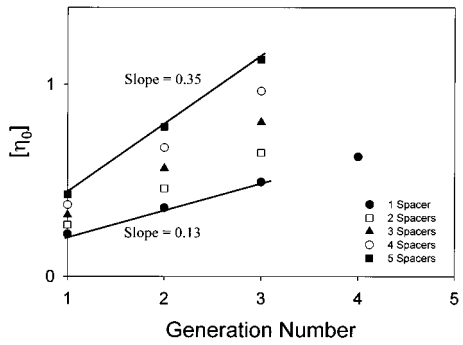

Figure 7. Effect of linear spacers on the dependence of intrinsic viscosity on the generation number.

0.44 for generation 1, from 0.42 to 0.55 for generation 2, and from 0.44 to 0.53 for generation 3. Increasing the number of spacers not only results in a rise in the magnitude of the zero-shear intrinsic viscosity but also results in a stronger dependence on the generation number as evidenced in Figure 7. This behavior is consistent with the simulation results of Lyulin et al.[13]

While the addition of spacers does increase the fraction of linear segments in the molecules, it also causes an increase in the molecular weight. To isolate the effects of molecular architecture on the rheology, it is necessary to separate out the molecular weight contribution. We have attempted to do this by performing simulations on a series of constant molecular weight structures with varying ratios of linear segments to branch points, spanning the extremes of the perfectly branched structure and the completely linear chain. Three sets of constant molecular weight systems, containing 30, 66, and 138 beads, respectively, were considered. A facet of our model is that, even in the most compact, perfectly branched configuration, one still has linear spring units which connect the trumbbells. In fact, the total number of springs in the above structures is exactly one less than the number of trumbbells. Except for the core trumbbell, each trumbbell has an associated connecting spring. The trumbbell and spring unit together are considered a single branching unit, which yields the following definition for x, the average number (or mole) fraction of additional linear units in the chain,

$$x = \frac{N_{spr} - N_{tr} + 1}{N_{spr} + 1} \tag{14}$$

For the perfectly branched structure, $x = 0$, and for a linear chain, $x = 1$.

Figure 8 shows the zero shear viscosity as a function of the mole fraction of additional linear segments for each of the three constant-bead systems. Perhaps the most important message of this paper comes from the observation that, for all three molecular weights, the transition from the low viscosity of the perfectly branched structure to the high viscosity of the linear chain occurs at a critical value of x. We further quantify this "transition" by looking at the x value when the viscosity rises by 20% of the difference between the viscosities at the two extremes. These viscosities are represented by the dashed lines in Figure 8, parts a−c. We find that in all cases the transition takes place at a mole fraction of linear segments around 0.8.

The 66-bead structures shown in Figure 9, parts a and b, both consist of 14 trumbbell units. They have

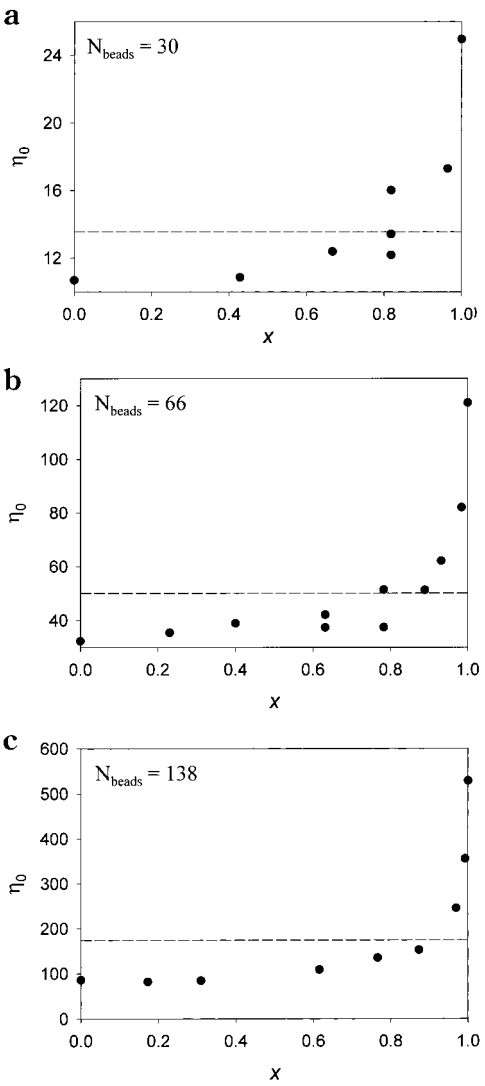

Figure 8. (a) Dependence of zero shear viscosity on the mole fraction of linear segments for the 30 bead system.The dashed line corresponds to a rise in viscosity that is 20% of the difference in viscosities of the $x = 0$ and $x = 1$ molecules. (b) Dependence of zero shear viscosity on the mole fraction of linear segments for the 66 bead system. (c) Dependence of zero shear viscosity on the mole fraction of linear segments for the 138 bead system.

identical molecular weights and the same mole fraction of linear segments of $x = 0.632$, but they differ in architecture. This phenomenon is known as "geometric isomerism". Flory[22] has calculated that for a branched polymer with a degree of polymerization of "n" and a B-group functionality of "f", the number of possible isomeric configurations is

$$\frac{nf!}{(nf - n + 1)!n!} \tag{15}$$

For a molecule made up of just 10 monomer units of AB_2 type, the number of possible configurations is 1.68×10^4. Clearly, it is intractable to account for every single possible isomer. However, valuable rheological information is obtained by looking at the few symmetric structures representative of a given ratio of linear segments to branch points. The structure in Figure 9b is found to exhibit a lower zero-shear viscosity than the one in Figure 9a. When the spring units are distributed toward the outside of the molecule as in Figure 9b, a

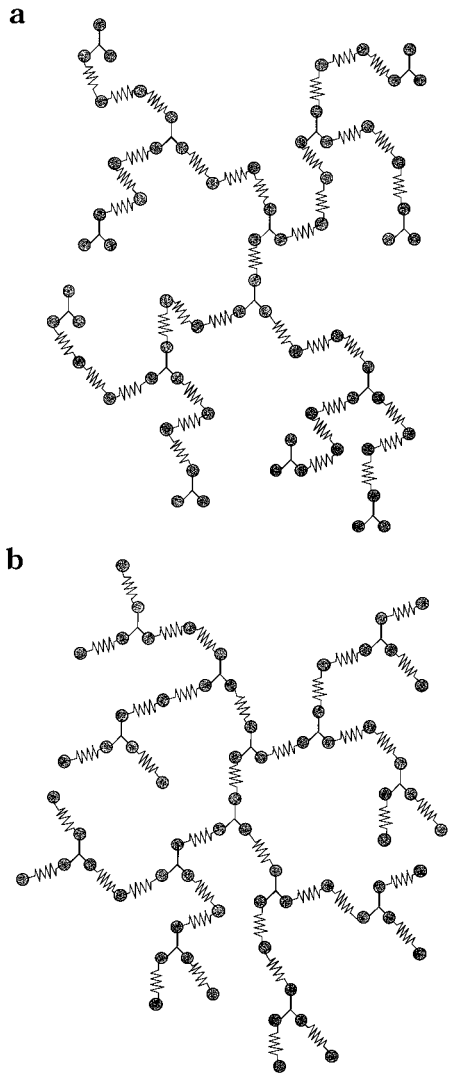

Figure 9. 66-bead molecules exhibiting "geometric isomerism". Both structures (a) and (b) contain identical numbers of spring and trumbbell units.

more compact structure with lower viscosity is obtained. As can be seen from Figure 8, parts a and b, two other sets of geometric isomers are encountered at $x = 0.818$ for the 30-bead system and $x = 0.783$ for the 66-bead system. In all cases, the lowest viscosities are observed for the structures where the linear segments are distributed among a greater number of branch points.

The sharp rise in zero-shear viscosity at $x = 0.8$ has been observed experimentally by Markoski et al.,[9] for a series of AB/AB_2 polyetherimide(PEI) copolymers of roughly identical molecular weights. Recently, Aerts[23] has utilized a Monte Carlo scheme, which accounts for variable reactivity of the second functional group, to generate AB/AB_2 copolymer structures of different ratios. However, a rigorous kinetic theory analysis is not performed and the intrinsic viscosity is calculated from the generated radius of gyration through the formula

$$[\eta] = \left(\frac{10\pi}{3}\right) \times R_g^3/M_w \qquad (16)$$

The completely linear structure has a viscosity that is roughly 4 times that of the $x = 0$ structure for the 66 bead system, the experimentally studied dilute solution (0.1 g/mL) PEI system[9] and Aerts' 249 bead system.

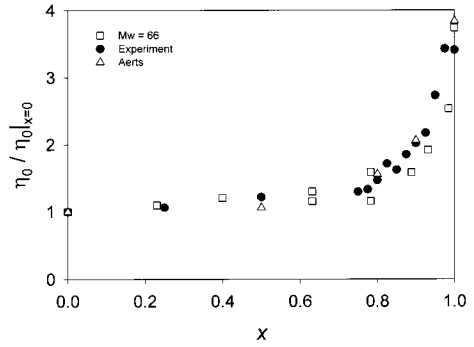

Figure 10. Scaled viscosity data of the 66 bead system plotted with the 249 bead system of Aerts[23] and the dilute solution (0.1 g/mL) experimental data of Markoski et al.[9]

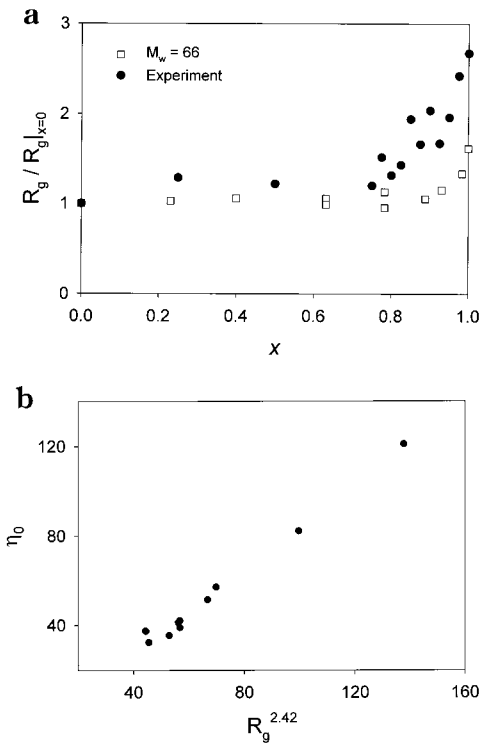

Figure 11. (a) Dependence of radius of gyration on the mole fraction of linear segments for the 66 bead system, plotted with the dynamic light scattering results of Sendijarevic et al.[10] (b) Power law relationship between zero shear viscosity and radius of gyration for the 66 bead system.

These viscosities scaled by their respective $x = 0$ values are plotted in Figure 10. A very close agreement is found between the transition trends of the three systems, with all the data points following a master curve.

The zero-shear radius of gyration values for the 66 bead system are plotted alongside the dynamic light scattering results of Sendijarevic et al. in Figure 11a. The radius of gyration is found to undergo a transition similar to that of the zero-shear viscosity, with a sharp transition beyond $x = 0.8$. This is consistent with the well-known fact that more compact structures correspond to lower viscosities. As seen in Figure 11b, a power law relationship, with a coefficient of 2.42, is found to hold for the 66 bead system. The experimental R_g undergoes a steeper transition with x and the experimental viscosity is found to follow a weaker $R_g^{1.35}$ dependence. The viscosity is found to scale as $R_g^{2.76}$ and $R_g^{1.85}$ for the 30 and 138 bead systems respectively (not shown). Kinetic theory studies of the Rouse chain have shown that for a large number of beads, the intrinsic

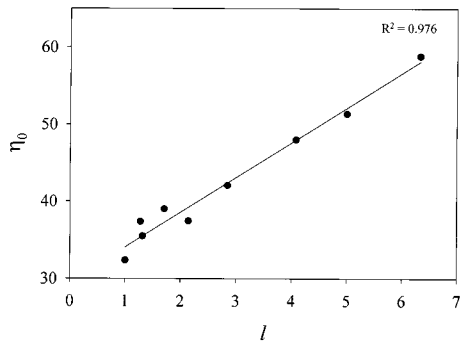

Figure 12. Zero shear viscosity vs average number of linear segments between branch points, for the 66 bead system.

viscosity scales as R_g^4/M, where M is the molecular weight. The inclusion of hydrodynamic interactions yields the Zimm chain, and the intrinsic viscosity is found to scale as R_g^3/M. Several theories[22] lead to the idea of an R_g^3/M scaling, and this is the most widely used relationship for linear chain polymers. While the same expression has been used to calculate intrinsic viscosities of hyperbranched polymers,[23] our more rigorous kinetic theory calculations indicate that such a simple relationship may not be accurate for the branched systems.

The experimental study of Markoski et al.[9] also demonstrated that the "average number of linear segments between branch points", l, determined from the copolymerization relations given by Frey et al.,[24] correlated linearly with the zero-shear viscosity. l represents the arithmetic average of the number of links between branch-points and between branch-points and end-points. For example, in the structure shown in Figure 9a, there are 12 stretches where there are three links between trumbbell units and there is one stretch with just one link between the trumbbells. Hence, the arithmetic average number of linear segments between branch points is $(12 \times 3 + 1 \times 1)/13 = 2.846$. As seen in Figure 12, the simulated zero shear viscosities also correlate linearly with l in these systems.

The extensional flow results are shown in Figure 13, parts a and b. At a low dimensionless extension rate of $\epsilon^* = 0.01$, the extensional viscosity is found to be roughly 3 times the zero shear viscosity for all three molecular weight systems. This is analogous to the behavior of Rouse/Zimm linear chain systems which are known to follow Trouton's rule at the lower extension rates. At a dimensionless extension rate of 10, much higher magnitudes of extensional viscosity are observed. In the linear systems, the extensional viscosity is known to scale as the fully extended end-to-end chain length at the higher elongation rates.[16] Since the molecules with a greater fraction of linear segments are more open and capable of unraveling, we find a marked increase in the extensional viscosity with x.

Conclusions

In this paper, we have performed Brownian dynamics simulations of several mixed linear-dendritic molecules utilizing a free-draining bead−spring−trumbbell model. The first normal stress difference is found to be more sensitive to the addition of spacers in the perfectly branched architecture. Our study of constant molecular weight hyperbranched systems with varying mole fractions of linear segments has led us to conclude that the transition from branched polymerlike properties to linear-chain-like properties occurs only beyond a mole fraction of around 0.8, in line with the experimental observations of Markoski et al.[9] Even the introduction of a very small number of branch points in a linear polymer can result in a significant reduction in size and viscosity. Our results are also in very close agreement with the experimentally observed behavior of the AB/AB_2 polyetherimide copolymers.[10]

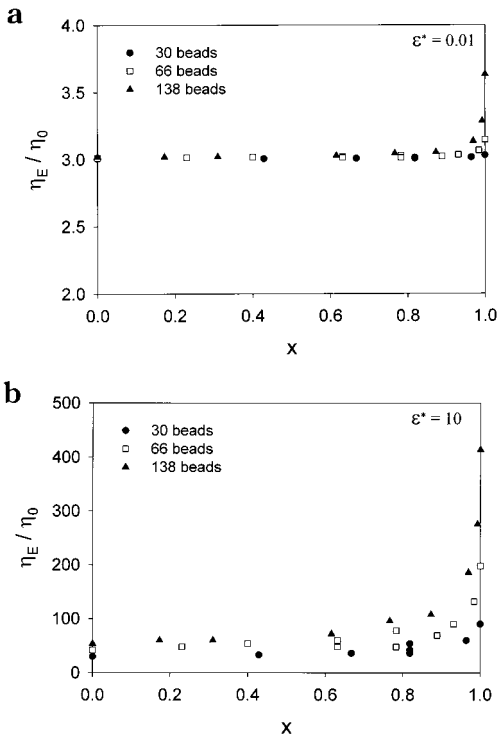

Figure 13. (a) Elongational viscosity scaled by the zero shear viscosity at a dimensionless extension rate of 0.01. (b) Elongational viscosity scaled by the zero shear viscosity at a dimensionless extension rate of 10.

Acknowledgment. This work has been supported under a grant from the U.S Army Research Office under Contract/Grant DAAG55-97-0126.

References and Notes

(1) Garbassi, F.; Gila, L.; Proto, A. *Polym, News* **1994**, *19* (12), 367.
(2) Schellekens, M. A. J.; Klumperman, B. *Macromol. Sci., Rev. Macromol. Chem. Phys.* **2000**, *C40* (2 & 3), 167.
(3) Buhleier, E.; Wehner, W.; Vogtle, F. *Synthesis* **1978**, 155.
(4) Tomalia, D. A.; Baker, H.; Dewald, J.; Hall, M.; Kallos, G.; Martin, S.; Roeck, J.; Ryder, J.; Smith, P. *Polym. J.* **1985**, *17*, 117.
(5) Newkome, G. R.; Yao, Z.; Baker, G. R.; Gupta, V. K. *J. Org. Chem.* **1985**, *50*, 2004.
(6) Wooley, K. L.; Hawker, C. J.; Frechet, J. M. J. *J. Am. Chem. Soc.* **1991**, *113*, 4252.
(7) Kim, Y. H.; Webster, O. W. *Polym. Prepr. (Am. Chem. Soc., Div. Polym. Chem.)* **1990**, *29*, 310.
(8) Sendijarevic, I.; McHugh, A. J. *Macromolecules* **2000**, *33*, 590.
(9) Markoski, L. J.; Moore, J. S.; Sendijarevic, I.; McHugh, A. J. *Macromolecules* **2001**, *34*, 2695.
(10) Sendijarevic, I.; McHugh, A. J.; Markoski, L. J.; Moore, J. S. *J. Rheol.*, in press.
(11) Lee, A. T.; McHugh, A. J. *Macromol. Theor. Simul.* **2001**, *10*, 244.
(12) Lee, A. T.; McHugh, A. J. *Macromol. Theor. Simul.* **2001**, *10*, 430.
(13) Lyulin, A. V.; Davies, G. R.; Adolf, D. B. *Macromolecules* **2000**, *33*, 3294.
(14) Andrews, N. C.; Doufas, A. K.; McHugh, A. J. *Macromolecules* **1998**, *31*, 3104.
(15) Murat, M.; Grest, G. S. *Macromolecules* **1996**, *29*, 1278.

(16) Bird, R. B.; Curtiss, C. F.; Armstrong, C.; Hassager, O. *Dynamics of Polymeric Fluids*; John Wiley and Sons: New York, 1987; Vol. 2.
(17) Hagerman, P. J.; Zimm, B. H. *Biopolymers* **1981**, *20*, 1481.
(18) Andrews, N. C.; McHugh, A. J.; Schieber, J. D. *J. Rheol.* **1998**, *42*, 281.
(19) Liu, T. W. *J. Chem. Phys.*, **1989**, *90*, 5826.
(20) Lescanec, R. L.; Muthukumar, M. *Macromolecules* **1990**, *23*, 2280.
(21) Curtiss, C. F.; Bird, R. B.; Hassager, O. *Adv. Chem. Phys.* **1976**, *35*, 31.
(22) Flory, P. J. *Principles in Polymer Chemistry*; Cornell University Press: Ithaca, NY, 1953.
(23) Aerts, J. *Comput. Theor. Polym. Sci.* **2000**, *10*, 73.
(24) Frey, H.; Holter, D. *Acta Polym.* **1999**, *50*, 67.

MA0103122